





Passive Lower Limb Exoskeleton for Kneeling and Postural Transition Assistance With Expanded Support Polygon

Sojiro Sugiura , Yaonan Zhu , *Member, IEEE*, Jian Huang , *Senior Member, IEEE*, and Yasuhisa Hasegawa , *Member, IEEE*

Abstract—Robotic exoskeletons, which assist in stand-to-kneel and kneel-to-stand (STK-KTS) movements and static kneeling postures are in great demand in the nursing field. This movement involves continuous adjustment of the center of gravity without a sufficient support polygon, which enhances the required joint effort of the ankle and knee. This study proposes a novel passive lower limb exoskeleton to support the movement. The exoskeleton was attached to the right leg and comprised a gas spring. The design followed an assistive strategy of the expanded support polygon. During the STK-KTS, the gas spring provided extra contact with the ground, thereby expanding the support polygon to increase motion stability and propping the knee to provide torque to the leg. The effectiveness of the gas spring was analyzed using a Lagrange dynamics-based simulation. Moreover, it was confirmed that the support polygon was expanded due to the proposed exoskeleton in real-world experiments. Further, experiments with seven healthy subjects showed that the exoskeleton reduced the time-integrated myoelectric potentials of the legs during STK-KTS (13.6%) and static posture (37.9%). These results imply that the proposed exoskeleton has the potential to reduce physical loads and provide a comfortable working environment for nursing workers.

Manuscript received 6 December 2022; revised 9 April 2023 and 29 May 2023; accepted 3 July 2023. Recommended by Technical Editor C. Liu and Senior Editor W. J. Chris Zhang. This work was supported in part by JST Moonshot RD under Grant JPMJMS2034Japan, International Science and Technology Cooperation Program of China under Grant 2017YFE0128300, and in part by the International Science and Technology Cooperation Program of Hubei under Grant 2021EHB003. (Corresponding author: Sojiro Sugiura.)

This work involved human subjects or animals in its research. Approval of all ethical and experimental procedures and protocols was granted by Ethics Review Committee of the relevant departments on the Higashiyama Campus of Nagoya University under Application No. 21-5, and performed in line with the Ethics of Research Involving Human Subjects.

Sojiro Sugiura, Yaonan Zhu, and Yasuhisa Hasegawa are with the Department of Micro-Nano Mechanical Science and Engineering, Nagoya University, Nagoya 464-8601, Japan (e-mail: sugiura@robo.mein.nagoya-u.ac.jp; zhu@robo.mein.nagoya-u.ac.jp; hasegawa@mein.nagoya-u.ac.jp).

Jian Huang is with the Key Laboratory of Image Processing and Intelligent Control, School of Artificial Intelligence and Automation, Huazhong University of Science and Technology, Wuhan 430074, China (e-mail: huang_jan@mail.hust.edu.cn).

This article has supplementary material provided by the authors and color versions of one or more figures available at <https://doi.org/10.1109/TMECH.2023.3294255>.

Digital Object Identifier 10.1109/TMECH.2023.3294255

Index Terms—Exoskeleton, lower limb support, stand-to-kneel and kneel-to-stand (STK-KTS) movement, work assistance.

I. INTRODUCTION

IN THIS article, physical workloads caused by forced static postures and repetitive posture transitions present musculoskeletal disorders in caregivers [1]. Dressing assistance is a common task for caregivers and forces them to bend their waist or maintain a kneeling posture [2], [3]. Several technologies have been developed to assist elderly people or physically challenged patients in dressing/undressing their clothes without the assistance of caregivers. In particular, some robots that hold a shirt and cooperate with the patient who sits on a chair or a bed to complete the dressing/undressing task have been developed [4], [5], [6]. However, the assistance of the robots is limited to dressing/undressing the clothes of the upper body. Dressing/undressing the clothes of the lower limb and shoes is still difficult for the robots because the task requires more interaction and contact with the patients. Therefore, dressing/undressing the clothes of lower limbs and shoes remains a job that needs caregivers' assistance.

In this task, caregivers manipulate their hands and the clothes near a floor and transfer from standing to working posture repeatedly, which will lead to a high burden on their lower limbs. Therefore, a device that supports the working posture performed near the floor and the transition movement is of great importance to caregivers. In addition, wearable-type assistance should be helpful for caregivers because each caregiver is responsible for dressing multiple patients and frequently moves between patient rooms.

Exoskeletons are wearable assistance devices and have been accepted in some working fields, such as industry, nursing care, and rehabilitation [7], [8], [9]. Generally, exoskeletons are designed as articulated robots with links attached to the body of the wearer and are divided into two categories depending on the assistive components: active and passive [10], [11]. Active exoskeletons use actuators and power supplies to assist the wearer and require high-level control systems while passive exoskeletons use only passive parts, such as springs, dampers, or brakes [12], [13]. Although active exoskeletons for rehabilitating injured or disabled people have been extensively researched,

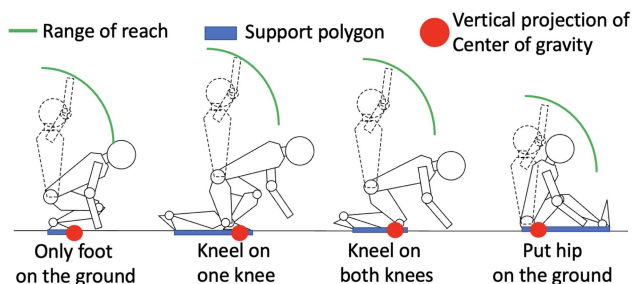


Fig. 1. Four possible postures to work near the floor.

TABLE I
COMPARISON OF FOUR POSSIBLE POSTURES

	Transition	Range of reach	Stability
Only foot on the ground	Easy	Medium	Unstable
Kneel on one knee	Easy	Large	Stable
Kneel on both knee	Difficult	Large	Stable
Put hip on the ground	Difficult	Small	Stable

their application to industrial or nursing care services is still at an experimental stage owing to their high cost, sophisticated structures, and battery capacity [7], [14]. On the other hand, passive exoskeletons have been utilized in some fields due to the low cost, simplicity of use, and no external power supply [10], [15], [16]. Therefore, we focused on a passive exoskeleton for caregivers who assist in dressing/undressing tasks.

Passive exoskeletons that support prolonged static postures have been developed in the last several years. A chairless chair was designed to assist workers who spend extended periods in a standing posture [15]. Similarly, Kawahira et al. [16] developed Archelis as an exoskeleton to support the standing position of doctors during surgery. These exoskeletons were reported to reduce the muscle load on the lower limb. However, these exoskeletons cannot assist the wearers with performing manual tasks near the floor, and they do not target the assistance of postural transition.

This study considers four possible postures taken by the caregivers performing the task and determines, which posture our exoskeleton should assist. In the scenario of dressing/undressing a patient's clothes, there are four possible postures: only foot on the ground, kneel on one knee, kneel on both knees, and the hip on the ground (see Fig. 1). These postures were compared from three aspects: ease of transition, range of reach, and stability. Table I gives which postures have advantages in which respect. First, postures that require fewer motion processes to complete the postural transition from a standing posture can be ideal. Kneeling on one knee and only foot on the ground need fewer motion processes compared with the other postures. Second, a larger range of reach can be helpful to complete dressing/undressing both upper body and lower limb clothes. The range of reach in the case of kneeling posture is large. Finally, choosing a stable posture will relieve the design requirement to stabilize the working posture. Fig. 1 shows a range of support polygons and a vertical projection of the center of gravity (CoG). A support polygon is defined as an area consisting of all grounding points. The closer the vertical projection of the CoG is to the side of the support polygon, the more unstable it is. The

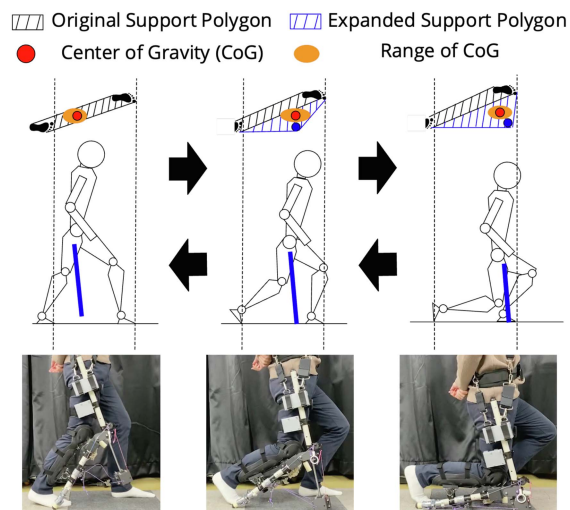


Fig. 2. Proposed novel assistive strategy "expanded support polygon" with an elastic brace (blue bar). The prototype to realize the assistive strategy is shown.

posture only foot on the ground can be the least stable, whilst the other postures keep high stability. Therefore, this article focuses on kneeling on one knee from three aspects. Moreover, the exoskeleton assisting the kneeling posture has the potential to expand its application from the nursing field to industries. For example, kneeling on one knee has been reported as a common posture for floor layers and has been targeted for assistance using active components [17].

Chen et al. [17] developed an active exoskeleton capable of assisting the wearer with a static kneeling posture and dynamic squatting movements by directly providing torque to the joints of the wearer. However, because the dynamic movements involve careful adjustment of the CoG inside the support polygon, assisting only the torques on the joints of the wearer may be insufficient for successful transfer. Hence, a novel assistance strategy that increases motion stability during dynamic transitions is required.

The exoskeleton should fulfill the following design policies: a passive type exoskeleton to be accepted in nursing fields, supporting the posture of kneeling on one knee to relieve the burden to perform tasks near a floor, and assisting the postural transition of stand-to-kneel (STK) and kneel-to-stand (KTS) while enhancing motion stability. We developed a passive exoskeleton to support the static kneeling posture and assist the dynamic STK-KTS movement, as shown in Fig. 2. The support for the static posture is achieved by constraining the position of the thigh and relieving the effort of the knee joint. To assist the dynamic movement, a strategy that expands a support polygon of the wearer with a passive elastic brace is proposed (see Fig. 2).

The rest of this article is organized as follows. A gas spring is selected as the elastic brace through a Lagrange dynamics-based simulation conducted in Section II. The detailed mechanism is described in Section III. Further, the effectiveness of the exoskeleton is evaluated with myoelectric measurements in Section IV. Section V provides discussion. Finally, Section VI concludes this article.

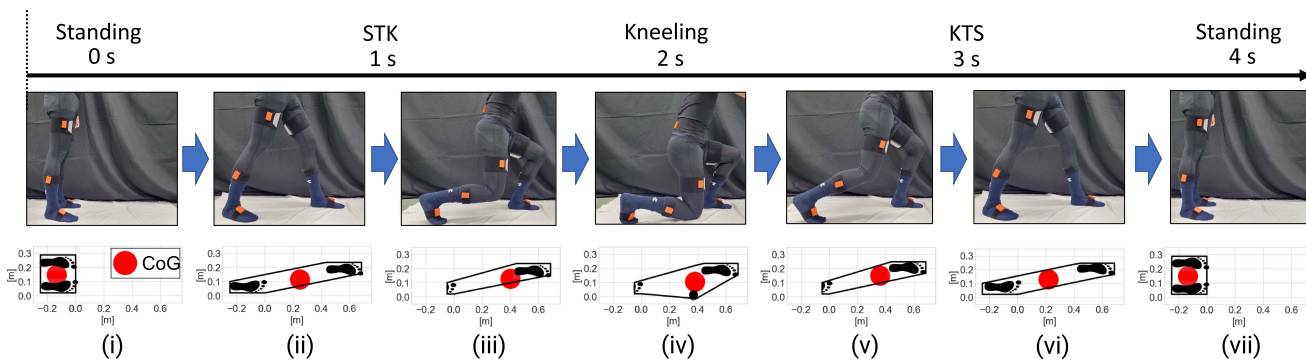


Fig. 3. STK-KTS procedure containing seven motions (i)–(vii). The CoG of the subject is the red circle.

The contributions of this study are summarized as follows.

- 1) A passive exoskeleton was designed to assist manual tasks in a kneeling posture. During the STK-KTS movement, an elastic brace attached to the thigh expands the support polygon of the wearer and enhances stability.
- 2) The effectiveness of the elastic brace was analyzed using a Lagrange dynamics-based simulation. The results showed that a gas spring was expected to efficiently assist the STK-KTS movements.
- 3) Experiments were performed with seven subjects for further validation. Myoelectricities of the lower limb muscles were measured and showed satisfactory results.

II. STK-KTS ANALYSIS AND ASSISTANCE REQUIREMENTS

This section analyzes the STK-KTS movement based on both real-world measurements and Lagrange dynamic-based simulations. These analyses provided a strategy of expanded support polygon, assistance requirements, and passive component selection.

A. STK-KTS Procedure and CoG Movement

During the STK-KTS movement, the vertical projection of the CoG moves around a side of the support polygon and renders maintaining balance a challenge. In this study, STK-KTS movement is defined as a sequence composed of seven phases: (i) standing, (ii) stepping forward with the left leg, (iii) shifting the CoG forward, (iv) maintaining the static kneeling posture, (v) lifting the CoG, (vi) shifting CoG backward, and (vii) returning to the standing posture, as shown in Fig. 3. Since these motions are asymmetric, we assumed that the right knee touches the ground in this study. The time interval to perform STK-KTS movement was investigated with six healthy subjects. They demonstrated STK-KTS movement at each comfortable speed, and all subjects performed STK-KTS between 3.5 and 4.0 s (average 3.69 ± 0.16). Hence, healthy people can perform STK-KTS within 4.0 s, and 4.0 s was decided as the time interval for simplicity in this article.

To confirm the difficulty in the motion, the vertical projection of the CoG and the range of the support polygon were measured with a motion capture system. A subject wore IMU-type motion

capture markers (Xsens) [18] and performed STK-KTS without any assistance. Fig. 3 shows the vertical projection of the CoG and the range of the support polygon during STK-KTS. It was confirmed that the CoG shifted up to the side of the support polygon from motion (ii) to (iii). Although CoG was inside the support polygon during motion (iv), it approached the side again during motion (v). Hence, it was estimated that motions (iii) and (v) were difficult to perform.

To enhance motion stability, this study considered two possible strategies: manipulating the CoG directly and expanding the support polygon. Since the position of the CoG is highly dependent on the posture, even a slight mistake in the manipulation of the CoG can cause falls of the wearer. In contrast, a slightly insufficient extension of the support polygons may not directly lead to a fall. Therefore, this study adopted a strategy of the expanded support polygon. The support polygon was expanded using an elastic brace (see Fig. 2) attached to one thigh in parallel, and the tip of the brace adds an extra grounding point.

To estimate the effectiveness of the strategy of expanded support polygon, we performed an additional analysis by calculating a margin for stability. This margin was obtained from the distance between the vertical projection of the CoG and the closest side of the support polygon. Fig. 4(a) and (b) shows the margin without and with the brace, respectively. The blue line represents the expanded support polygon with the brace, and the additional vertex was defined as the vertical projection of the right knee. Fig. 4(c) and (d) shows the margin during motion (iii) and (v), respectively. The margin without any assistance was continuously less than 5 cm, while with the brace it was more than 10 cm. Hence, these results showed that the expanded support polygon can increase the margin for stability during STK-KTS movement.

B. Dynamic Analysis of STK-KTS

To analyze the difficulty of STK-KTS from the view of the required joint efforts of the lower limb, a dynamic simulation using the Euler–Lagrange formalism was conducted [19]. A dynamic human model was employed and performed STK-KTS movement, as shown in Fig. 5. The human body was composed of three parts: shin, thigh, and HAT (head, arm, and torso). We assumed that the shin included the foot, and the toe joint was

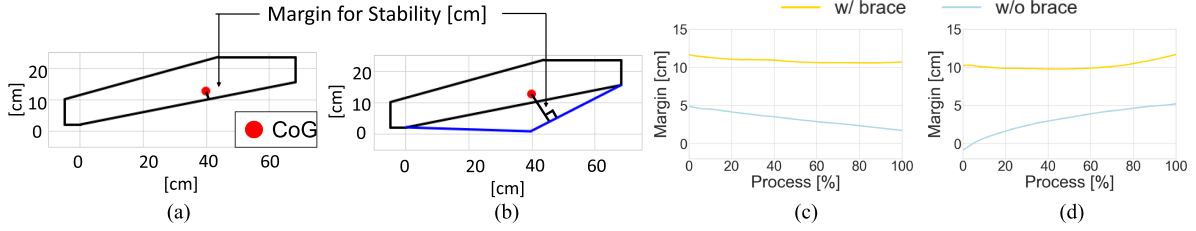


Fig. 4. Definition of the margin for stability and its results. (a) Margin without the brace. (b) Margin with the brace. The blue line refers to the expanded support polygon's sides. (c) Time-series data of the margin during motion (iii). (d) Time-series data of the margin during motion (v).

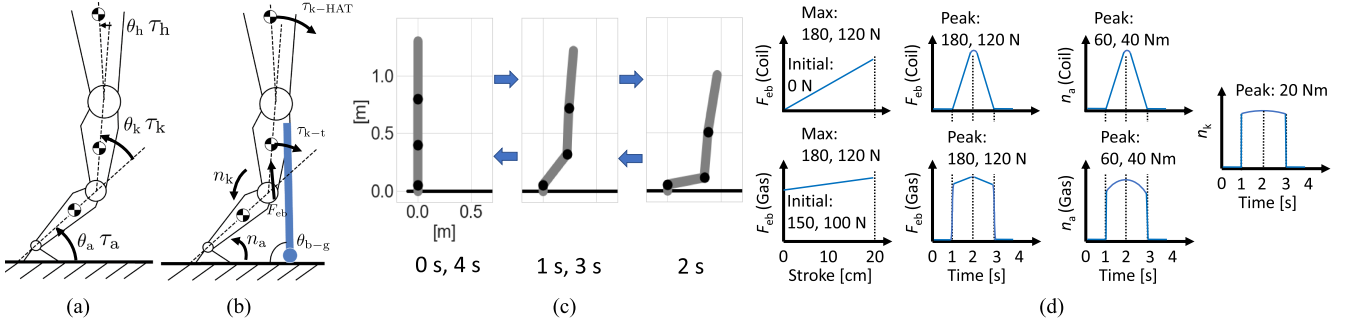


Fig. 5. Simulation setups. (a) Model of a human (wearer). (b) Model of a human and an elastic brace. (c) Model performs the STK movement in the first 2 s and the KTS movement in the following 2 s. (d) Spring force characteristics and assistive force (torque) generated by the elastic brace.

ignored. This simulation focused on only the right side of the body, to which the elastic brace was attached. Therefore, the human model was described as a triple-inverted pendulum [20]. The angles of the ankle, knee, and hip joints are represented as θ_a, θ_k , and θ_h , respectively [see Fig. 5(a)]. The length, mass, and moment of inertia were obtained from Leva's report [21]. We assumed that the wearer distributed the body weight on the right and left sides equally to maintain dynamic stability. The weight of the human model and that of the right side were assumed to be 60 and 30 kg, respectively. The Euler-Lagrange formalism for the human model is as follows:

$$M(\theta)\ddot{\theta} + C(\theta, \dot{\theta})\dot{\theta} + G(\theta) = U \quad (1)$$

where θ is the vector of $[\theta_a \ \theta_k \ \theta_h]^T$. M , C , and G are the mass matrix, Coriolis matrix, and the gravitational vector, respectively. U is the vector of the torque at which the joints of the human model require $[\tau_a \ \tau_k \ \tau_h]^T$.

Fig. 5(c) shows the model performing the STK-KTS transition. The commands of the joint angle θ were configured based on the trajectory of the human performing STK-KTS measured using a motion capture system.

We assumed that the human model performs postural transition by controlling the angle of the three joints θ . This study adopted a simplified proportional-differential (PD) feedback controller, while there are sophisticated methods for simulating human models, such as linear-quadratic regulator design [22] and fictitious gain [23]. This study considered that a simplified PD feedback controller ($K_p = 4000, K_d = 300$ [20]) applied to each joint can efficiently demonstrate the wearer's role and lead to intuitive insights regarding the performance of the STK-KTS. Fig. 6(a) shows that the angles of the joints θ were controlled

by the PD model. We consider that the PD model sufficiently tracked the command.

Fig. 6(b) shows the torque required by the joints θ . The torques reached a peak ($234 \text{ N} \cdot \text{m}$) at 1.2 s, and the large output continued till 2.6 s. In addition, the ankle and knee joints required large plantar flexion torque and knee flexion torque, respectively. Thus, as expected in Section II-A, large efforts were required in motions (iii) and (v).

C. Assistance Requirements and Simulation of Assistance

The assistance requirements of the STK-KTS movement were determined based on the result of the simulation. First, reducing the plantar flexion torque of the ankle joint is the major requirement due to the large output. Second, an assistance for the knee flexion torque is also necessary because large output was observed. Finally, our proposed exoskeleton should assist the lower limb from 1 to 3 s because the joints required a large torque continuously during the period.

The ankle joint can receive an assistive torque for plantar flexion from the elastic brace when the brace pushes the kneecap. Hence, the characteristic of the elastic brace can significantly influence the effectiveness of the assistance. To determine the suitable assistive component, additional dynamic simulation was conducted among various kinds of assistive braces. This simulation was conducted with four different elastic components: coil spring (maximum force is 120 N), coil spring (max 180 N), gas spring (max 120 N), and gas spring (max 180 N). The spring constants k of the springs were 600, 900, 100, and 150 N/m in order. The compression length was assumed 20 cm on every spring, and they were

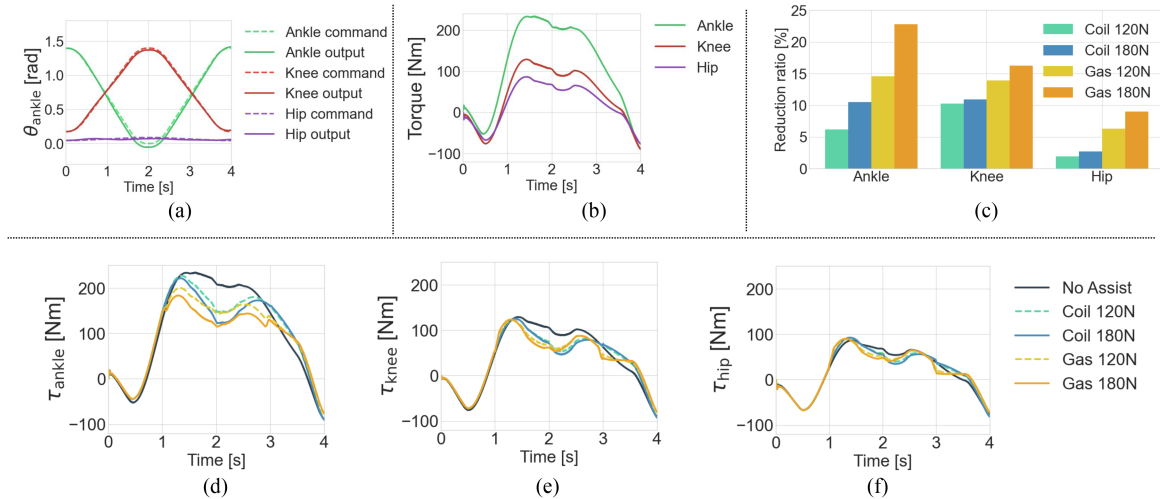


Fig. 6. Simulation results. (a) Time-series data of angle of each joint of the human model during the transition. Dot lines represent input commands of angle, and solid lines represent output of the model. (b) Torque required at each joint during STK-KTS without any assistance. (c) Reduction ratio of efforts in each joint over time in four assistive conditions. (d)–(f) Time-series data of torque that each joint required.

compressed at a constant speed (20 cm/s) in this simulation [see Fig. 5(d)].

A gas spring is a kind of gas cylinder that comprises a piston rod and a cylinder filled with gas. The reaction force of gas springs is constantly larger than that of coil springs [see Fig. 5(d)]. In addition, gas springs can be compressed smoothly compared with coil springs. Due to their smoothness, they are highly adaptable to ergonomics [24] and have been widely used in worker assistance [25], [26].

In this article, the maximum force of the springs was designed to be under 200 N. Since we assumed that the body weight is equally distributed on the right and left sides, concentrating more than half body weight on the right knee will make the right foot leave the ground and significantly enhance the fall risk. Further, the actual users' weight will range from 40 to 80 kg while this simulation uses a 60-kg human model. Given wearers whose weight is 40 kg, the maximum force should be designed to be less than 200 N (half of 400 N). In this study, 180 N was selected as the maximum assistive force from the low-cost and high-performance gas spring lineup: options for the maximum force are 240, 180, and 120 N.

To reduce the required efforts of the human model's knee joint, valid methods of assistance were discussed. The effort was caused because the torso and right thigh are always positioned in front of the right knee. Since the CoG moves around the side of the support polygon, the right knee needs to carefully adjust its joint angle to prevent the thigh and the torso from moving forward too much. Although the left leg grounds in front of the other body parts and supports the body weight, the instability remains due to the limited support polygon. Therefore, it is effective to apply torque to the right knee so that the thigh and torso do not move too far forward. In this simulation, this force was defined as a torque to compensate for the moment of the thigh and torso. This torque can be generated by mechanically constraining the relative position of the right thigh to the elastic brace during STK-KTS.

The human model was modified as a human-brace model [see Fig. 5(b)]. The weight of the exoskeleton (4.0 kg) was added to the weight of the human model's shin and thigh. In this simulation, damping elements of the springs were not taken into account for simplicity [26], [27]. The Euler-Lagrange formalism for the human-brace model is as follows:

$$M(\theta)\ddot{\theta} + C(\theta, \dot{\theta})\dot{\theta} + G(\theta) = U + N \quad (2)$$

where N denotes the vector of the assistive torque applied from the elastic brace to the human model's ankle and the knee $[n_a \ n_k \ 0]^T$. n_a was generated by the reaction force of the elastic brace and mainly assisted in driving the plantar flexion torque. n_k is produced as a reaction torque to prevent the thigh from moving forward direction too much. n_a and n_k are obtained as follows:

$$n_a = F_{eb} l_{shin} \cos\{\theta_{eb-g} - (\pi/2 - \theta_a)\} \quad (3)$$

$$n_k = -(\tau_{k-HAT} + \tau_{k-t}) \quad (4)$$

where F_{eb} is the assistive force from the elastic brace [see Fig. 5(d)], and l_{shin} is length of shin [21]. θ_{eb-g} is the angle between the elastic brace and the ground [see Fig. 5(b)]. Further, τ_{k-HAT} and τ_{k-t} are the torques acting on the knee joint generated by the weight of the HAT and thigh, respectively. The torques τ_{k-t} and τ_{k-HAT} make the thigh move forward, and n_k prevents the movement. The assistive torque N is applied from 1 to 3 s. Regarding the gas springs, we defined the rise and fall time as 0.1 s during 1.0–1.1 and 2.9–3.0 s, respectively, to make the force plot smooth. The time-series data of n_a and n_k are shown in Fig. 5(d).

Fig. 6(c) shows the reduction ratio of effort over time (EoT) in each condition and joint. EoT is defined as total efforts required during the time interval [28] and is obtained by integrating the absolute torque over time (4 s), as shown in the following:

$$EoT = \int_{t_1}^{t_2} |\tau| dt \quad (5)$$

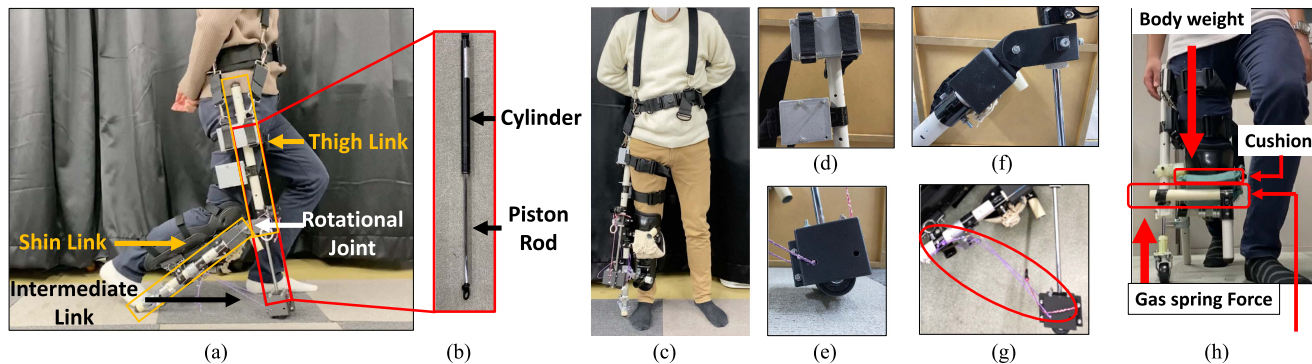


Fig. 7. Thigh brace exoskeleton (TBE). (a) Overview and the main parts. (b) Gas spring and its components. (c) Front view. (d) Two thigh belts. (e) Wheel attached to the tip of the gas spring. (f) Rotational joint. (g) Intermediate link. (h) Link propping the knee cap.

where τ means torque required in ankle, knee, or hip joints. In this simulation, t_1 and t_2 are 0 and 4 s, respectively. Fig. 6(d)–(f) shows the time-series data of torques required by the human model’s joints. Regarding the ankle joint, the required torque was reduced in every assistance condition [see Fig. 6(d)]. The gas springs succeeded in reducing the peak torque due to the initial large force compared with coil springs, and the gas spring (180 N) reduced EoT the most (22.8%). Therefore, it was expected that the gas spring (180 N) was the suitable elastic brace to reduce the required effort of the ankle joint. On the other hand, there were no gaps at 2 s if the maximum force of the springs is the same. However, it would not be a focal point because the springs have no role in reducing the torque in the static kneeling posture (2 s). Moreover, given that coil springs require linear guides for actual usage, gas springs have no disadvantages in terms of mass, cost, durability, or mechanism complexity [24]. Therefore, we designed the exoskeleton to assist the STK-KTS movement using the gas spring.

The flexion torque of the knee joint was reduced owing to the assistance, while the differences between the four assistive conditions were not significant. Hence, the torque n_k mainly reduced the knee flexion torque. To achieve this assistance, we need to design an exoskeleton that can constrain the relative position of the thigh to the gas spring.

III. MECHANICAL DESIGN AND ASSISTIVE STRATEGY

In this section, we introduce a prototype of the proposed exoskeleton and evaluate the strategy of the expanded support polygon.

A. Passive Lower Limb Exoskeleton

Based on the assistance requirements mentioned in Section II-C, a passive lower limb exoskeleton was developed, as shown in Fig. 7. This exoskeleton is referred to as thigh brace exoskeleton (TBE) for convenience. TBE was attached to the right thigh and shin, and it mainly assisted the right leg. TBE comprised two main links, gas spring, wheel, rotational joint, and intermediate link. The gas spring was selected as an elastic brace and expanded the support polygon by putting the tip on

the ground. The other parts had their role and contributed to the novel strategy of expanded support polygon.

The first link was attached to the thigh and is referred to as a thigh link [see Fig. 7(a)], which was attached by two belts that are referred to as thigh belts [see Fig. 7(d)]. The position of the thigh belts was adjustable, so the users could wear TBE according to their leg lengths. The second link was attached to the shin by a knee–shin guard and is referred to as a shin link [see Fig. 7(a)]. The links are steel plate cold commercial pipe. The gas spring was attached to the thigh link, which was in the pipe and covered the gas spring [see Fig. 7(b)]. The range of output was from 150 to 180 N linearly (the spring constant is 150 N/m). The rotational joint was connected to the thigh link and shin link [see Fig. 7(f)]. It had one degree of freedom and performed as though it was a knee joint. The intermediate link was a simple and strong wire [see Fig. 7(g)]. It was attached to the tip of the gas spring and the shin link. The length of this link has an important role to decide the trajectories of the thigh link during the STK-KTS. The wheel was attached to the tip of the gas spring [see Fig. 7(e)] and a soft cushion was attached to the knee–shin guard to relieve the pressure applied to the knee.

B. Design for Assistance Requirements

There are three requirements to assist STK-KTS movement, as mentioned in Section II-C. To satisfy the assistance requirements, various parts were incorporated into TBE.

First, the gas spring was used to assist the plantar flexion torque of the ankle joint. The thigh link was used to attach the gas spring to the thigh of the wearer, and the wheel helped the tip of the gas spring move on the ground smoothly. A pipe extending from the thigh link propped the knee cap to apply the assistive force to the lower limb [see Fig. 7(h)]. However, only these parts could not assist the plantar flexion torque because the wearer could not compress the gas spring at all owing to the movement of the wheel, while the wheel was necessary for smooth grounding. Furthermore, if the grounding point moves freely, the range of the support polygon becomes unstable, and the wearer may lose his balance. The main cause of this issue was that the movement of the wheel was not restricted. Hence,

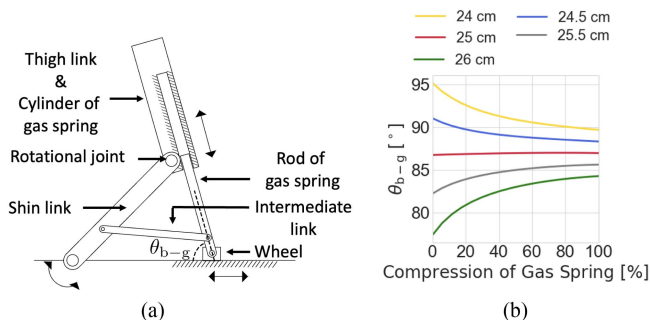


Fig. 8. (a) Link mechanism of TBE to constrain the trajectory of the gas spring. θ_{eb-g} is the angle between the brace (gas spring) and the ground. (b) Relationship between θ_{eb-g} and the compression ratio of the gas spring by the length of the intermediate link.

the issue was solved by constraining the postures of both the gas spring and the wheel.

To realize the constraint, a link mechanism was constructed using the shin link, the rotational joint, and the intermediate link, as shown in Fig. 8(a). We assumed that the tip of the shin link was fixed on the ground due to a friction force between the ground and the tip of the shin link. A rubber cap was attached to the tip. The rotation of the shin link around the tip led to the compression of the gas spring, and the intermediate link prevented the wheel from moving forward freely. The movement of the wheel was determined by the amount of compression of the gas spring, which means that the posture of TBE was uniquely decided by the rotation of the shin link. Due to the constraint, the trajectory of the grounding point was also determined uniquely, which means that the transformation of the support polygon became stable for every trial.

Second, the assistance requirement for the knee flexion torque can be satisfied by constraining the relative position of the thigh to the gas spring. The gas spring prevents the thigh from moving forward too much. The experiment conducted in Section II-A showed that the right thigh kept vertical to the ground from 1 to 3 s (see Fig. 3). It is considered that people can perform the STK-KTS comfortably if the thigh keeps the angle. Hence, the angle between the gas spring and the ground θ_{eb-g} should be designed to keep about 90°. Given the direction that the wheel moves, the angle should be between 85 and 90°. The range of the angle θ_{eb-g} changes according to the links' length, particularly the intermediate link. We conducted a parametric search about the length of the intermediate link and made θ_{eb-g} almost between 85 and 90°. Fig. 8(b) shows the relationship between θ_{eb-g} , the compression ratio of the gas spring, and the length of the intermediate link. A length of 25 cm was selected because the range remains around 87°.

Finally, to satisfy the requirement about the timing of assistance, the length of the gas spring's rod was determined as 20 cm. Although the length can be adjusted by people, 20 cm was used in this article to prepare for a unified experimental setup. We confirmed that 20 cm was enough to reduce the effort of the lower limb in Section IV.

Supporting the static kneeling posture is another requirement to enhance the effectiveness of TBE. To support the static

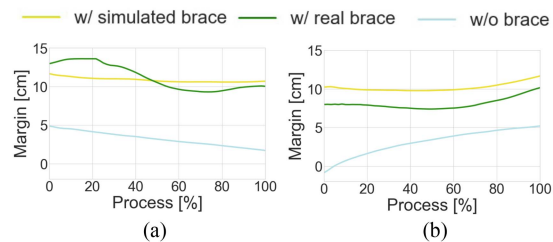


Fig. 9. (a) and (b) Time-series data of the margin during motion (iii) and (v), respectively. The blue and yellow lines are the same as Fig. 4, and the green line is an additional result performed with TBE.

kneeling posture, we focused on two points: postural oscillations and pressure. First, fast postural oscillations of the knee joint can be observed during the static kneeling [29], and the knee joint requires constant fine-tuning. Mechanical constraints of the thigh can prevent oscillations and relieve the effort of the lower limbs. Since the thigh link is in front of the thigh, forward falling is prevented. In addition, the thigh belts support the thigh from the back side, which constrains the angle of the knee joint. The effectiveness of relieving the effort is evaluated in Task 2 in Section IV. Second, the knee is exposed to considerable pressure from the ground [30]. The pressure can be relieved using a knee guard and soft cushion [31], as shown in Fig. 7.

C. Assistive Strategy of Expanded Support Polygon

TBE has the strategy of the expanded support polygon. The effectiveness of this strategy was analyzed through the same experiment conducted in Section II-A. The trajectory of CoG and the support polygon were measured with the motion capture system, and the margin for stability was calculated.

Fig. 9 shows that the margin with a real brace (TBE, green), with a simulated brace (result in Section II-A, yellow), and without any brace (blue). The margin with TBE was always more than 9 and 7 cm during motion (iii) and (v), respectively. It was confirmed that TBE expanded the support polygon during STK-KTS compared with the condition without any assistance. The average increments were 5.0 and 8.0 cm in motion (iii) and (v), respectively. Hence, this experiment confirmed that TBE successfully expanded the support polygon of the wearer during STK-KTS.

Compared with the result of the simulation conducted in Section II-A, the movement of CoG with a real TBE was unstable during motion (iii). It is considered that the use of TBE might change the weight applied to the right leg, which shifted the position of the CoG and make the distance unstable. Regarding the result of motion (v), the margin in the case of TBE was 2.1 cm less than that of the simulated brace. The differences could be caused because the simulation did not take into account the wearer's plan to reduce the joint effort. It is considered that the wearer shifted his CoG toward the grounding point of the gas spring and applied his weight to the gas spring, which reduced the body weight applied to his leg and relieves the joint efforts. On the other hand, the margin was reduced because the CoG approached the side of the support polygon. To confirm whether the amount of the expansion was enough to reduce the

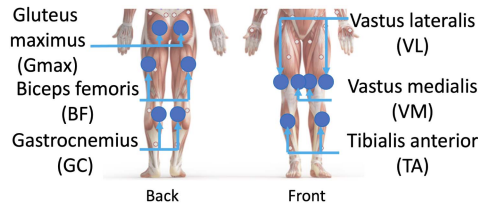


Fig. 10. Six kinds of muscles measured in the experiments.

wearer's effort, this study conducted another experiment about myoelectricity in Section IV.

IV. EXPERIMENTS

This section examines the basic performance of TBE based on the measurements of myoelectricity. The experiment was divided into three categories: STK-KTS movements, static kneeling posture, and task near the floor.

A. Participants

The participants were seven young men with no physical disabilities (24.4 ± 1.0 years, 172 ± 5.0 cm, 58 ± 9.5 kg). Consent was obtained from all participants before performing the experiments. This study was approved by the ethics committee of Nagoya University (No. 21-5).

B. Methods and Measurements of Myoelectric Potentials

The myoelectric potential was used to evaluate the effectiveness of the assistance. It is an electric signal that flows through muscle fibers when muscles contract [32]. This value enabled the quantitative evaluation of the performance of TBE. In this experiment, a noninvasive method was used to measure myoelectric potential using a wireless sensor (Cometa). The sampling frequency of the sensors was 2000 Hz. The acquired signals were passed through a 5–500 Hz band pass filter and smoothed using root mean square with a 0.1-s window. The total effort of the muscles over time was obtained by integrating the processed signals with time [28].

The following muscles were measured on the right and left sides, as shown in Fig. 10: gluteus maximus, biceps femoris (BF), vastus lateralis (VL), vastus medialis (VM), tibialis anterior (TA), and gastrocnemius (GC). These muscles were selected based on biological articles on squatting [33].

Further, % maximum voluntary contraction (% MVC) was used to normalize the measured myoelectric potential. MVC is a method to decrease the influence of muscle size among subjects. The subjects performed MVC on each muscle for 3 s in specific postures, with an interval of 1 min. The postures were determined based on Konrad [32]. The data was assessed using a paired-sample *t*-test, and significant gaps are represented by * ($p < 0.05$) and ** ($p < 0.01$).

C. Procedures

Since the purpose of these experiments is to evaluate the basic performance of TBE, experiments on each function were conducted separately.

First, Task 1 was conducted to confirm the effectiveness of the transition assistance. The subjects performed the STK-KTS movements under two conditions: with TBE [see Fig. 11(a)] and without TBE [see Fig. 11(b)]. The transition of both STK and KTS required 2 s each. The subjects practiced completing this movement in just 2 s using a metronome. Since the total effort of the muscles was acquired by integrating with time for the same duration, a slight difference in the speed could be minimized. The subjects repeated the movements five times. In the condition without TBE, a pad was set on the ground to match the height of TBE when the subjects were kneeling [see Fig. 11(b)].

Second, Task 2 was carried out to confirm TBE reduced the effort of the lower limb in the static kneeling posture. The subjects maintained a kneeling posture with and without TBE for 30 s, as shown in Fig. 11(c) and (d). The same setup as in Task 1 was used to match the height of the knee. To investigate the effect of the thigh belts that constrained the knee joint angle, another condition was added: the subjects maintained the kneeling posture with TBE but without the thigh belts, as shown in Fig. 11(e). The results of this task would indicate whether the wearer can complete tasks such as dressing/undressing patients' upper body clothes.

Finally, the subjects engaged in Task 3, which was conducted to confirm whether TBE can assist with dressing/undressing tasks done near the floor. The subjects performed a manual task near the floor for 30 s in two conditions: (f) kneeling with TBE and (g) kneeling without TBE, as shown in Fig. 11(f) and (g). In this task, the subjects were asked not to support their body with their upper limbs to measure the effort of the lower limb properly.

Each subject practiced the tasks for 30 min before starting the experiments, and all subjects were accustomed to TBE. The tasks were done in order, and the order of conditions in each task was randomized.

D. Results

It was found that TBE reduced the myoelectric potential during STK-KTS movements, particularly in the right leg, as shown in Fig. 12(i). The mean reduction was 2.2% MVC ($p < 0.05$) and the reduced EoT was 13.6%. The reduction on the right side was 4.1% MVC ($p < 0.05$). Further, the largest decrease was 9.1% MVC in the right VL ($p < 0.05$), followed by 6.5% MVC in the same VM ($p < 0.05$) and 4.1% MVC in the same TA ($p < 0.05$). In contrast, the left-side muscles showed a 0.4% MVC reduction. No significant difference due to the body size was observed in this task.

Fig. 12(ii) shows myoelectric potential during the static kneeling posture. Regarding the comparison between cases (c) with TBE and (d) without TBE, the average reduction in myoelectric potential was 2.9% MVC ($p < 0.01$), and the reduction of EoT was 37.9%. In addition, the reduction in the right leg was 3.2% MVC ($p < 0.05$). The reduction in the right VL muscle was 8.2% MVC ($p < 0.05$), which was the largest of all the measured muscles in this task. Subsequently, the reduction in the right TA was 4.2% MVC ($p < 0.01$). Regarding the difference between (c) with TBE and (e) with TBE but without thigh belts, it was observed that the condition of no belts increased the output in the right VL and VM muscles by 3.7% and 3.2% MVC, respectively.

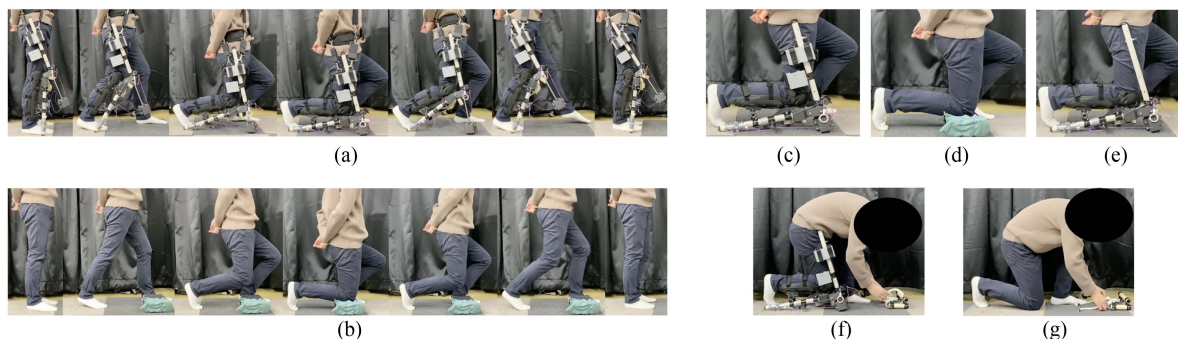


Fig. 11. Postures demonstrated in the experiments. Task 1: (a) with TBE and (b) without TBE. Task 2: (c) with TBE, (d) without TBE, and (e) with TBE but without the thigh belts. Task 3: (f) with TBE, and (g) without TBE.

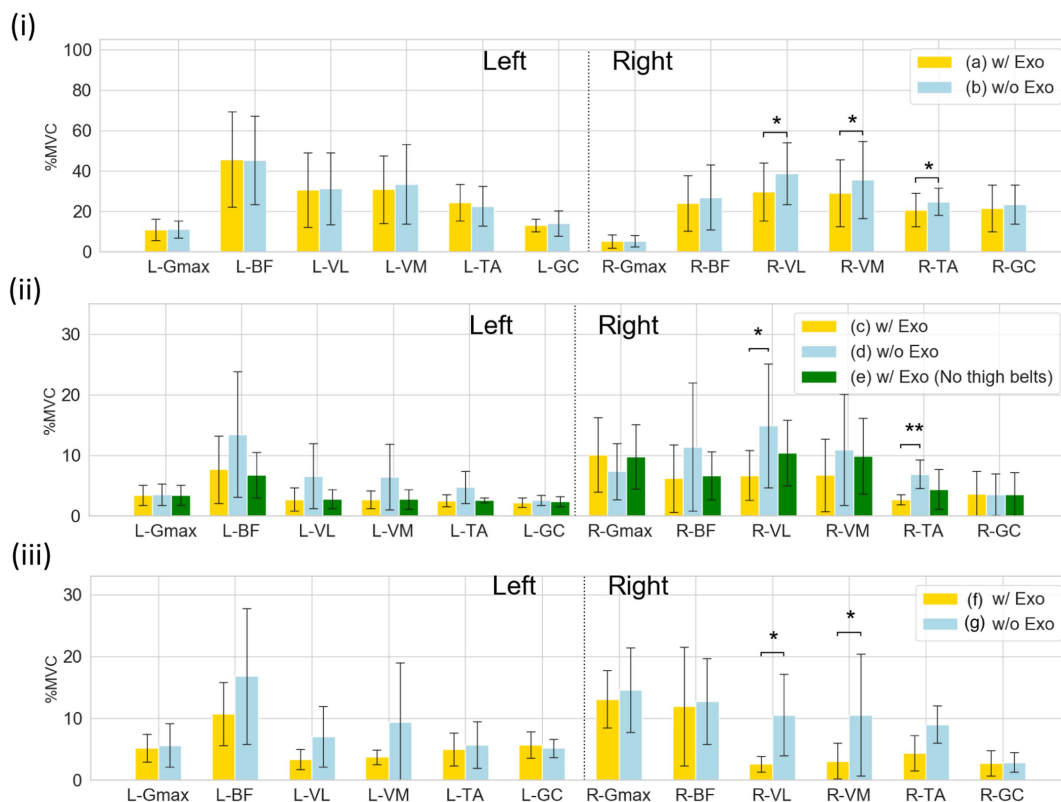


Fig. 12. Total effort of the myoelectric potential divided by 100% MVC. Error bars indicate standard deviation. (i) Task 1: STK-KTS movements, (ii) Task 2: Static kneeling posture, and (iii) Task 3: Work near the floor.

TBE reduced myoelectric potential during the tasks near the floor, as shown in Fig. 12(iii). The average reduction was 3.2% MVC, and a significant difference was observed in the right leg ($p < 0.05$). The right VL and VM recorded 8.0% MVC ($p < 0.05$) and 7.5% MVC ($p < 0.05$) reduction, respectively.

V. DISCUSSION

A. STK-KTS Movements

The experiments confirmed that TBE reduced the myoelectric potential of the wearer during the STK-KTS movements [see Fig. 12(i)]. The reduction on the right side was greater than that on the left side because TBE was attached only to the right leg.

Large reductions were observed in the right VL and VM [see Fig. 12(i), R-VL, and R-VM]. Because the output of these muscles could be decreased by the improved stability of CoG [34], the strategy of the expanded support polygon could be effective.

Furthermore, the reduction of the right BF muscle, which is responsible for the knee flexion torque, was not significant. This could be because the effect of the force applied to the thigh to prevent the forward fall was too small to reduce the effort of the knee torque. This indicates that another elastic part is needed to reduce the muscle activity.

A significant reduction was observed in the right TA, which works for the dorsal flexion of the ankle joint. On the other hand, the activity of the right GC muscle, which works for the plantar

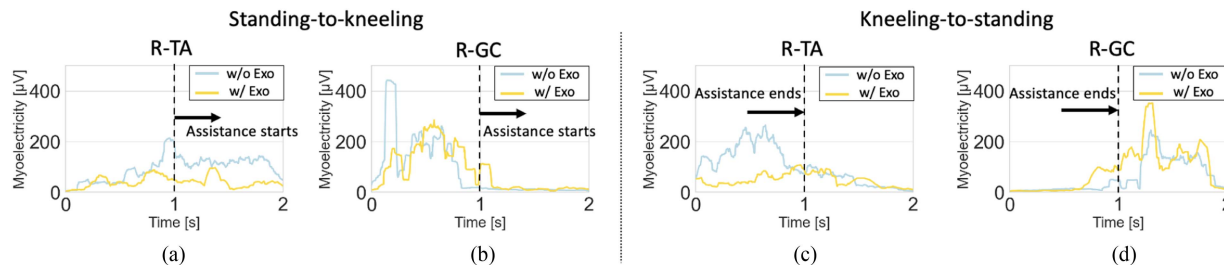


Fig. 13. Myoelectric potential of the right TA and GC muscles of one subject. Yellow and blue lines represent values with TBE and without TBE. (a) and (b) Time-series data of the muscle activities from standing to kneeling postures in right TA and GC muscle, respectively. (c) and (d) Time-series data from kneeling to standing postures in right TA and GC muscle, respectively.

flexion of the ankle joint, was not reduced significantly, although it was expected that the GC muscle activity would be reduced by TBE.

Fig. 13 shows the time-series data of the myoelectricity in the right TA and GC muscles, and the GC muscle did not work during the period when TBE assisted (1–2 s during STK and 0–1 s during KTS). In addition, as shown in Fig. 11(a) and (b), the subject performed STK-KTS by changing his knee and toe joints, not the ankle joint. We considered that the subject enhanced the motion stability by fixing one joint and reducing the number of joints to be controlled. That indicates that the ankle joint was fixed during the assistance, and there was no difference in the activity of the GC muscle when TB assisted the wearer.

On the other hand, the TA muscle worked hard when TBE was not worn, as shown in Fig. 13. It is considered that the TA muscle was required to fix the angle rather than the GC muscle because the angle was fixed at the maximum dorsal flexion position. When TBE assists the movement, TBE expands the support polygon of the wearer and enhances the stability, which could relieve the efforts of the fixation and reduce the TA muscle activity. We considered the relief led to the reduction of the TA muscle activity.

The results indicate the enhanced stability owing to the expanded support polygon reduced the muscle activities of the right VL, VM, and TA muscles. The amount of the expansion investigated in Section III-C was sufficient. Furthermore, since the reduction in BF and GC muscle activities was limited, we should analyze the kinematics and biomechanics of STK-KTS in the future. For the analysis, it would be essential to use the optical motion captures for measuring the movement of the knee, ankle, and toe joints more accurately.

B. Static Kneeling

TBE reduced the myoelectric potential of the leg during the static kneeling posture. Large reductions were observed in the right VL and TA [see Fig. 12(ii), R-VL, and R-TA]. We considered that these muscles were used to constrain the knee joint, and TBE could relieve the effort.

To ensure the effect on the constraint of the knee joint, the condition of the kneeling posture with TBE, but without thigh belts [see Fig. 11(e)] was examined. It was observed that myoelectricity in the right VL, VM, and TA muscles [see

Fig. 12(ii-e), R-VL, R-VM, and R-TA] increased when the thigh belts were removed. This indicates that the constraint of the knee joint worked well and assisted the wearer in maintaining a static kneeling posture.

The activities of the left BF, VL, VM, and TA muscles were also reduced. Thus, the right leg could afford to support the left leg, owing to assistance in the right leg. However, in contrast to the activity of the right muscles, the activity of the left muscles was not affected by the thigh belts [see Fig. 12(ii-c) and (ii-e)].

Through the task, it was confirmed that TBE could reduce the muscle activities of the lower limbs in the kneeling posture. These results confirmed that caregivers could dress/undress patients' upper body clothes in the kneeling posture with reduced muscle effort.

C. Task Near the Floor

In the experiment simulating the manual task near the floor, TBE reduced the myoelectric potential of the legs. Large reductions were observed in the right VL, VM, and TA muscles [see Fig. 12(iii), R-VL, R-VM, and R-TA]. As in Task 2, the thigh belt is expected to contribute to the reduction. Similar results to Task 2 were obtained for left muscle output.

In Section I, it was mentioned that an exoskeleton that can assist caregivers in dressing/undressing patients' lower limb clothes near the floor is required. The results of this experiment indicate that the wearer can complete tasks done near the floor without large muscle activities owing to TBE.

VI. CONCLUSION

This study developed a lower limb exoskeleton, TBE, which assisted in the transition of STK-KTS and the static kneeling posture. The movements require physical effort due to the shift of the CoG. Consequently, TBE assisted the wearer in movements by employing a novel strategy of expanding the support polygon. Through analysis with Lagrange dynamics, it was confirmed that TBE reduced the required torque of the leg during STK-KTS movements.

Experiments were conducted to investigate the performance of TBE. The myoelectric potentials of the legs during the STK-KTS transition were reduced owing to the use of TBE. Since appropriate assistive force can depend on the user's weight, an investigation into the assistive force and body weight will be conducted in the future. TBE also reduced muscle output in

the static kneeling posture. The constraint on the knee joint was confirmed to have contributed to this reduction. When subjects worked near the floor with TBE, the load on the leg was reduced. Therefore, these results imply that TBE assists caregivers in comfortably doing tasks done near the floor, such as dressing/undressing patients' clothes and shoes. Moreover, TBE has the potential to prevent caregivers from injuries/disorders due to manual work. In the future, the effects of using TBE for long periods will be verified at real sites, such as nursing houses.

One limitation of TBE is the size. Although the wearer can walk while wearing TBE, going through a narrow area should be difficult. Transformation mechanisms, such as folding would be effective to avoid the conflict between the exoskeleton and environments during walking. We will conduct detailed stress analysis and mechanical optimization to reduce the size of TBE while maintaining durability.

Since lower back pain is another issue for caregivers, developing a function supporting lower back would be also helpful. In the future, we will focus on a more comprehensive exoskeleton capable of reducing the load of the low back in addition to the lower limbs.

REFERENCES

- [1] J. A. Engels, J. Van Der Gulden, T. F. Senden, and B. van't Hof, "Work related risk factors for musculoskeletal complaints in the nursing profession: Results of a questionnaire survey," *Occup. Environ. Med.*, vol. 53, no. 9, pp. 636–641, 1996.
- [2] Q. V. Doan et al., "Relationship between disability and health-related quality of life and caregiver burden in patients with upper limb poststroke spasticity," *PMR*, vol. 4, no. 1, pp. 4–10, 2012.
- [3] W. Burleson et al., "An assistive technology system that provides personalized dressing support for people living with dementia: Capability study," *JMIR Med. Informat.*, vol. 6, no. 2, 2018, Art. no. e5587.
- [4] Y. Gao, H. J. Chang, and Y. Demiris, "User modelling for personalised dressing assistance by humanoid robots," in *Proc. IEEE/RSJ Int. Conf. Intell. Robots Syst.*, 2015, pp. 1840–1845.
- [5] Z. Erickson, H. M. Clever, G. Turk, C. K. Liu, and C. C. Kemp, "Deep haptic model predictive control for robot-assisted dressing," in *Proc. IEEE Int. Conf. Robot. Autom.*, 2018, pp. 4437–4444.
- [6] F. Zhang, A. Cully, and Y. Demiris, "Probabilistic real-time user posture tracking for personalized robot-assisted dressing," *IEEE Trans. Robot.*, vol. 35, no. 4, pp. 873–888, Aug. 2019.
- [7] S. Yeem, J. Heo, H. Kim, and Y. Kwon, "Technical analysis of exoskeleton robot," *World J. Eng. Technol.*, vol. 7, no. 1, pp. 68–79, 2018.
- [8] Y. Zhu, T. Ito, T. Aoyama, and Y. Hasegawa, "Development of sense of self-location based on somatosensory feedback from finger tips for extra robotic thumb control," *Robomech J.*, vol. 6, no. 1, pp. 1–10, 2019.
- [9] D. F. Paez-Granados, H. Kadone, M. Hassan, Y. Chen, and K. Suzuki, "Personal mobility with synchronous trunk–knee passive exoskeleton: Optimizing human-robot energy transfer," *IEEE/ASME Trans. Mechatron.*, vol. 27, no. 5, pp. 3613–3623, Oct. 2022.
- [10] T. Bosch, J. van Eck, K. Knitel, and M. de Looze, "The effects of a passive exoskeleton on muscle activity, discomfort and endurance time in forward bending work," *Appl. Ergonom.*, vol. 54, pp. 212–217, 2016.
- [11] H. Lee, W. Kim, J. Han, and C. Han, "The technical trend of the exoskeleton robot system for human power assistance," *Int. J. Precis. Eng. Manuf.*, vol. 13, no. 8, pp. 1491–1497, 2012.
- [12] R. Chaichaowarat, V. Macha, and W. Wannasuphprasit, "Passive knee exoskeleton using brake torque to assist stair ascent," in *Proc. IEEE Region 10 Conf.*, 2020, pp. 1165–1170.
- [13] J. Kim, J. Kim, Y. Jung, D. Lee, and J. Bae, "A passive upper limb exoskeleton with tilted and offset shoulder joints for assisting overhead tasks," *IEEE/ASME Trans. Mechatron.*, vol. 27, no. 6, pp. 4963–4973, Dec. 2022.
- [14] T. Yan, M. Cempini, C. M. Oddo, and N. Vitiello, "Review of assistive strategies in powered lower-limb orthoses and exoskeletons," *Robot. Auton. Syst.*, vol. 64, pp. 120–136, 2015.
- [15] T. Luger, R. Seibt, T. J. Cobb, M. A. Rieger, and B. Steinhilber, "Influence of a passive lower-limb exoskeleton during simulated industrial work tasks on physical load, upper body posture, postural control and discomfort," *Appl. Ergonom.*, vol. 80, pp. 152–160, 2019.
- [16] H. Kawahira, R. Nakamura, Y. Shimomura, T. Oshiro, and S. Okazumi, "Clinical use of a wearable lower limb support device for surgeries involving long periods of standing," *J JSCAS*, vol. 20, no. 3, pp. 121–125, 2018.
- [17] S. Chen et al., "Wearable knee assistive devices for kneeling tasks in construction," *IEEE/ASME Trans. Mechatron.*, vol. 26, no. 4, pp. 1989–1996, Aug. 2021.
- [18] A. Karatsidis, G. Bellusci, H. M. Schepers, M. De Zee, M. S. Andersen, and P. H. Veltink, "Estimation of ground reaction forces and moments during gait using only inertial motion capture," *Sensors*, vol. 17, no. 1, 2016, Art. no. 75.
- [19] J. J. Craig, *Introduction to Robotics: Mechanics and Control, 3/E*. Prentice Hall: Pearson Educ. India, 2009.
- [20] W. Huo et al., "Impedance modulation control of a lower-limb exoskeleton to assist sit-to-stand movements," *IEEE Trans. Robot.*, vol. 38, no. 2, pp. 1230–1249, Apr. 2022.
- [21] P. de Leva, "Adjustments to Zatsiorsky-Seluyanov's segment inertia parameters," *J. Biomech.*, vol. 29, no. 9, pp. 1223–1230, 1996.
- [22] A. M. Mughal and K. Iqbal, "Physiological LQR design for postural control coordination of sit-to-stand movement," *Cogn. Comput.*, vol. 4, no. 4, pp. 549–562, 2012.
- [23] K. Kong and M. Tomizuka, "Control of exoskeletons inspired by fictitious gain in human model," *IEEE/ASME Trans. Mechatron.*, vol. 14, no. 6, pp. 689–698, Dec. 2009.
- [24] O. MONROE, "The benefits of gas springs: What you should know," Accessed: Jul. 16, 2023. [Online]. Available: <https://monroeengineering.com/blog/the-benefits-of-gas-springs-what-you-should-know/>
- [25] Y. Hasegawa, T. Hoshino, and A. Tsukahara, "Wearable Assistive Device for Physical Load Reduction of Caregiver-Adaptive to Caregiver's Motion During Transferring Support," in *Proc. IEEE World Autom. Congr.*, 2016, pp. 1–6.
- [26] J. Hull, R. Turner, and A. T. Asbeck, "Design and preliminary evaluation of two tool support arm exoskeletons with gravity compensation," *Mechanism Mach. Theory*, vol. 172, 2022, Art. no. 104802.
- [27] Y. Zhu, G. Zhang, H. Li, and J. Zhao, "Automatic load-adapting passive upper limb exoskeleton," *Adv. Mech. Eng.*, vol. 9, no. 9, 2017, Art. no. 1687814017729949.
- [28] R. Chaichaowarat, D. F. P. Granados, J. Kinugawa, and K. Kosuge, "Passive knee exoskeleton using torsion spring for cycling assistance," in *Proc. IEEE/RSJ Int. Conf. Intell. Robots Syst.*, 2017, pp. 3069–3074.
- [29] R. A. Mezzarane and A. F. Kohn, "Postural control during kneeling," *Exp. Brain Res.*, vol. 187, no. 3, pp. 395–405, 2008.
- [30] Y. Wang, Y. Fan, and M. Zhang, "Comparison of stress on knee cartilage during kneeling and standing using finite element models," *Med. Eng. Phys.*, vol. 36, no. 4, pp. 439–447, 2014.
- [31] H. Xu, S. Jampala, D. Bloswick, J. Zhao, and A. Merryweather, "Evaluation of knee joint forces during kneeling work with different kneepads," *Appl. Ergonom.*, vol. 58, pp. 308–313, 2017.
- [32] P. Konrad, "The ABC of EMG," *A Practical Introduction Kinesiological Electromyography*, vol. 1, no. 2005, pp. 30–35, 2005.
- [33] V. C. Dionisio, G. L. Almeida, M. Duarte, and R. P. Hirata, "Kinematic, kinetic and EMG patterns during downward squatting," *J. Electromyogr. Kinesiol.*, vol. 18, no. 1, pp. 134–143, 2008.
- [34] A. S. Aruin, W. R. Forrest, and M. L. Latash, "Anticipatory postural adjustments in conditions of postural instability," *Electroencephalogr. Clin. Neurophysiol./Electromyogr. Motor Control*, vol. 109, no. 4, pp. 350–359, 1998.



Sojiro Sugiura received the B.S. degree in mechatronics in 2020 from the Department of Mechanical System Engineering of Nagoya University, Japan, and the M.S. degree in mechatronics in 2022 from the Department of Micro-Nano Mechanical Science and Engineering, Nagoya University, Nagoya, Japan, where he is currently working toward the Ph.D. degree in robotics with the Department of Micro-Nano Mechanical Science and Engineering.

His research interests include wearable robotics and mechanical designs.



Yaonan Zhu (Member, IEEE) received the B.S. degree in automation from Northeastern University, Shenyang, China, in 2015, the M.S. degree in computer science from the University of Science and Technology of China, Hefei, China, in 2018, and the Ph.D. degree in robotics from Nagoya University, Nagoya, Japan, in 2021.

He is currently a Designated Assistant Professor with Nagoya University. His research interests include telerobotics and teleoperation, haptics and haptic interfaces, human-centered

robotics, and wearable robotics.



Yasuhisa Hasegawa (Member, IEEE) received B.E., M.E., and Ph.D. degrees in robotics from Nagoya University, Nagoya, Japan, in 1994, 1996, and 2001, respectively.

From 1996 to 1998, he was with Mitsubishi Heavy Industries, Ltd., Tokyo, Japan. In 1998, he joined Nagoya University. In 2003, he joined Gifu University, Gifu, Japan, in 2003. From 2004 to 2014, he was with the University of Tsukuba, Tsukuba, Japan. Since 2014, he has been with Nagoya University, where he is currently a Professor with the Department of Micro-Nano Mechanical Science and Engineering. His research interests include motion-assistive systems, teleoperation, and surgical robots.

robotics, and surgical robots.



Jian Huang (Senior Member, IEEE) received the B.S. degree in automatic control engineering, the M.E. and Ph.D. degrees in control science and engineering from the Huazhong University of Science and Technology (HUST), Wuhan, China, in 1997, 2000, and 2005, respectively.

From 2006 to 2008, he was a Postdoctoral Researcher with the Department of Micro-Nano System Engineering and the Department of Mechano-Informatics and Systems, Nagoya

University, Nagoya, Japan. He is currently a Full Professor with the School of Artificial Intelligence and Automation, HUST. His research interests include rehabilitation robots, robotic assembly, networked control systems, and bioinformatics.